Microsecond Laser Ablation of Thrombus and Gelatin Under Clear Liquids: Contact Versus Noncontact

HanQun Shangguan, Lee W. Casperson, *Fellow, IEEE,* and Scott A. Prahl

***Abstract*— Laser thrombolysis is a procedure for removing blood clots in occluded arteries using pulsed laser energy. The laser light is delivered through an optical fiber to the thrombus. The ablation process is profoundly affected by whether the optical fiber tip is inside a catheter or is in contact with the thrombus. This study measured ablation efficiency of 1-μs laser pulses to remove a porcine clot confined in a silicone tube. The cavitation process was investigated by visualizing laser-induced bubble formation on gelatin targets with flash photography and measuring the acoustic transients with a pressure transducer. The laser spot size did not affect the mass of material removed. The efficiency of the contact ablation was at least three times greater than that of the noncontact ablation. Finally, the mass removed was closely correlated with the measured bubble expansion pressure.**

I. Introduction

LASER thrombolysis is a promising method for management of vessels blocked by thrombus such as occurs during acute myocardial infarction and stroke [1]. Laser thrombolysis uses laser pulses to clear arteries obstructed by thrombus (blood clots). The laser pulses generate cavitation bubbles in a blood vessel through the absorption of laser energy by a target (e.g., blood clot) or surrounding liquids (e.g., blood and saline). The bubbles expand and collapse within a millisecond of the delivery of the laser pulse and disrupt the thrombus. Safety is achieved by using laser wavelengths that are relatively strongly absorbed by the blood clot as compared to absorption by the vessel wall [2]–[4].

During laser thrombolysis, the laser pulses are delivered to the blood clot using an optical fiber whose tip either contacts or does not contact the clot. The contact method has been used with excimer lasers (308 nm) and mid-infrared lasers (2.1 μm) [5], [6]. Ablation occurs at the tip during such procedures. If a fluid-core optical catheter is used to wash away ambient blood, then visible wavelength laser pulses can ablate the clot in a noncontact manner [7].

Previous studies have demonstrated that the ablation processes are quite different for contact and noncontact methods [8]–[12]. Srinivasan *et al.* demonstrated that contact excimer laser ablation of plaque was more violent than noncontact ablation when the same energy was used [8]. Gijsbers *et al.* reported a dramatic increase in ablation efficiency when the optical fiber contacted porcine aortic tissue [9], and that the ablation depth increased with increasing force between the fiber face and the tissue [12]. Similar results have also been reported by Buchelt *et al.* [11]. No detailed study of contact and noncontact delivery on the ablation efficiency has been reported, although many studies have demonstrated that ablation efficiency depends on pulse energy [4], [13], radiant exposure [11], [14], [15], pulse duration [15], properties of the tissue [16], repetition rate [17], and fiber contact pressure [9], [11], [12].

It is difficult to precisely position the fiber-optic catheter *in vivo* and this paper investigated the consequences of inadvertent contact of the fiber with the thrombus. When the fiber does not contact the thrombus, the radiant exposure depends on the distance between the thrombus surface and the fiber end due to the divergence of the laser beam. The laser energy may also be attenuated by the absorption of the surrounding medium. These effects are eliminated when the fiber end contacts the thrombus surface. Since contact ablation is more efficient than noncontact ablation, we measured the pulse energies required to achieve the same material removal for the two modalities.

We measured the ablation efficiency of 1-μs, 577-nm laser pulses on a porcine clot confined in a silicone tube. Laser energies ranging from 10 to 75 mJ were delivered through 200–400-μm optical fibers. The ablated mass was determined by weighing the samples before and after ablation. We visualized the bubble formation with flash photography and measured acoustic transients with a pressure transducer. These experiments were performed on gelatin-based thrombus models. The use of this thrombus model provided a reproducible substrate for modeling thrombus ablation. Finally, we also evaluated contact and noncontact methods for localized drug delivery.

II. Materials and Methods

A. Sample Preparation

1) Porcine Clot: Fresh nonheparinized blood was obtained from domestic swine and immediately placed into cylindrical

Manuscript received October 1, 1996; revised November 8, 1996. This work was supported in part by the Murdock Foundation, Portland, OR, and the Whitaker Foundation, Washington, DC.

H. Q. Shangguan is with the Department of Electrical Engineering, Portland State University, Portland, OR 97201 USA, and the Oregon Medical Laser Center, Portland, OR 97225 USA.

L. W. Casperson is with the Department of Electrical Engineering, Portland State University, Portland, OR 97201 USA.

S. A. Prahl is with the Oregon Medical Laser Center, Portland, OR 97225 USA, and the Oregon Health Sciences Univesity, Portland, OR 97201 USA.

Publisher Item Identifier S 1077-260X(96)09600-1.

1077–260X/96$5.00 © 1996 IEEE

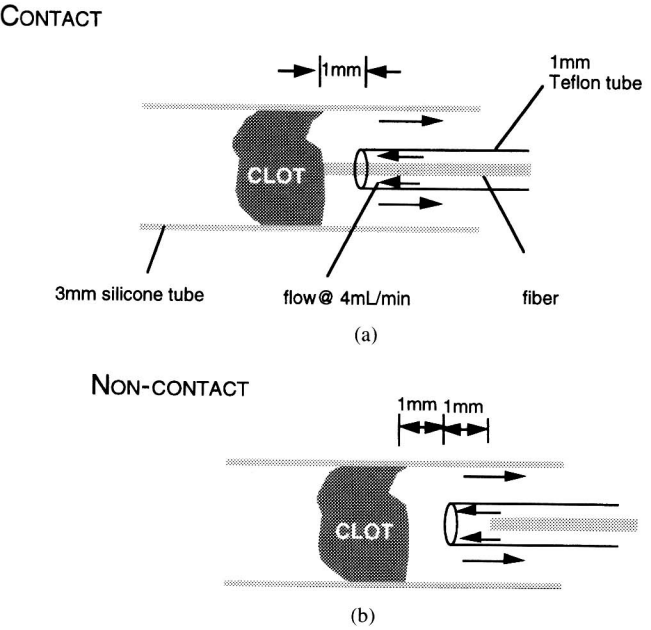

g. 1. Schematic of contact and noncontact ablation experiment. In both ses, clear fluid flows out of the catheter at 4 mL/min to wash debris away om the ablation site.

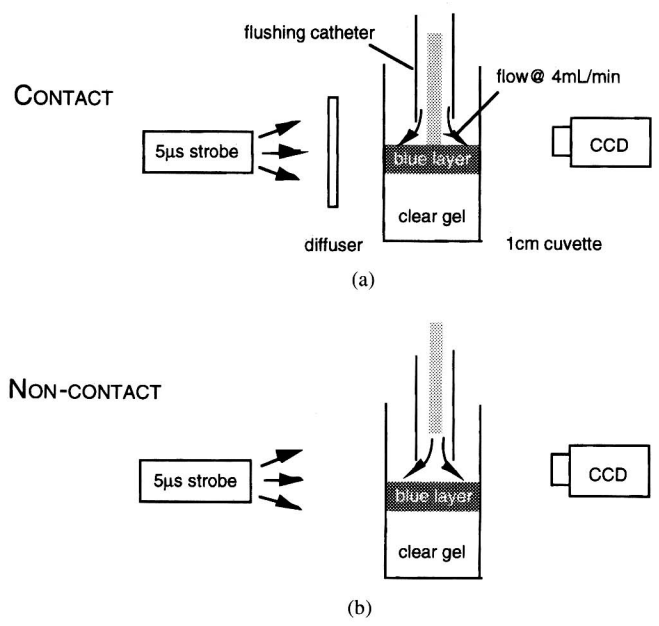

Fig. 2. Experimental setup for the visualization of cavitation bubble formation. The blue layer was 300 μm thick and had an absorption coefficient of 100 cm^{-1}.

ass tubes. The blood was allowed to clot at room temperature r 5 h and then stored at 8 °C for 24 h. The durability the clot varied from pig to pig; more white fibrin pieces ere found in the most durable samples. The clots were cut to pieces ~10 mm long, ~2 mm wide, and ~2 mm thick. hey were weighed using a digital balance with a precision ±100 μg (AE200, Mettler) and then confined in a silicone be (Fig. 1). The tube had a 3-mm inner diameter and a all thickness of 0.4 mm. The mechanical properties differed om those of human arteries; the Young's modulus of the icone tube was 8 N/mm^2, whereas it is 2–5 N/mm^2 for man vessels [18]. The clot samples from three different pigs ere ablated to assess the intra-animal variation of clot on the lation efficiency.

2) *Gelatin Targets:* A thrombus model consisted of 3.5% 5 bloom gelatin (Sigma). The percentage was determined by e weight ratio of gelatin to water. The bloom number is the ndard method for indicating the toughness of gelatins and is measure of surface tension. Higher bloom numbers indicate onger gelatins. No attempt was made to correlate the bloom mber with the strength of any specific clots in this study. The latin-water mixture was heated to 60 °C with stirring until became clear. Two types of gelatin targets were formed in m cuvettes. Flash photography used a clear gelatin substrate vered by a thin layer of absorbing gelatin. These were de by pouring clear liquid gelatin in 1-cm cuvettes and ng to form 2–3 cm thick targets with flat surfaces. A dye lution (0.07 g of Blue 15 from Sigma in 40 mL water) s placed on the gelatin surface for five min. and a blue er about 300 μm thick with an absorption coefficient of 00 cm^{-1} (at 577 nm) was formed. This blue layer allowed boundaries of the cavitation bubble to be seen, even when y otherwise would have been hidden by a light absorbing atin substrate (Fig. 2). Pressure measurements and drug delivery experiments both used a uniformly absorbing gelatin target made by adding 0.07 g of Blue 15 to 40 mL of liquid gelatin and curing. The 100 cm^{-1} blue gelatins were carefully removed from the cuvettes and cut into ~5-mm thick sections before the experiments.

B. Laser Delivery

All experiments used a flashlamp-pumped dye laser (Palomar Medical Technologies) operating at 577 nm. The pulse duration was 1.3 μs (full width at half maximum). The laser energy was determined using a joulemeter (Molectron). Contact experiments used 10–25 mJ/pulse; noncontact experiments used three times as much. Pulse-to-pulse energy variation was less than 5%. The repetition rate was 3 Hz for the ablation efficiency measurements. The laser pulses were delivered through a flushing catheter that consisted of a single 200–400-μm step-index fused-silica optical fiber contained inside a 1-mm flexible Teflon tube. The fiber tip extended 1 mm from the distal end of the catheter during contact delivery; the tip was 1 mm inside the catheter during noncontact delivery (see Fig. 1). Distilled water or normal saline was injected through the Teflon tube with a syringe infusion pump (Harvard Apparatus) at a flow rate of 4 mL/min to wash away the removed clot or gelatin from the target site. The fiber tip always slightly contacted the targets (clot or gelatin) during contact delivery and was 2 mm from the target surfaces during noncontact delivery. The spot size on the target surface was obtained from the burn pattern on a deep-dyed polyester film. The spot sizes were 200, 300, and 400 μm for contact ablation and 450, 480, and 520 μm for noncontact ablation. The laser beam profile on the target was nearly Gaussian for noncontact ablation, and had flat profile for contact ablation. The laser energy and spot sizes used in this study are summarized in Table I.

TABLE I

CONTACT AND NONCONTACT ABLATION EXPERIMENTS. THE MASS PER PULSE IS THE AVERAGE AMOUNT OF CLOT (FROM PIG B IN TABLE II) REMOVED IN A SINGLE LASER PULSE. THE BUBBLE SIZE AND PRESSURE MEASUREMENTS ARE FROM GELATIN ABLATION EXPERIMENTS. THE ERRORS VARY, BUT TYPICAL VALUES ARE SPECIFIED IN THE FIRST ROW

CONTACT DELIVERY					NON-CONTACT DELIVERY				
Pulse Energy (mJ)	Spot Size (μm)	Mass per Pulse (μg)	Bubble Size (mm)	Expansion Pressure (kPa)	Pulse Energy (mJ)	Spot Size (μm)	Mass per Pulse (μg)	Bubble Size (mm)	Expansion Pressure (kPa)
		±30	±0.1	±20			±30	±0.1	±30
10	200	130	—	—	30	450	—	—	—
	300	—	2.5	110		480	100	3.1	130
	400	130	—	—		520	70	—	—
15	200	170	—	—	45	450	—	—	—
	300	—	2.7	190		480	160	3.3	210
	400	150	—	—		520	100	—	—
20	200	160	—	—	60	450	140	—	—
	300	170	2.8	230		480	160	3.6	270
	400	140	—	—		520	150	—	—
25	200	210	—	—	75	450	—	—	—
	300	—	2.9	310		480	250	3.7	330
	400	210	—	—		520	180	—	—

C. Ablation Efficiency Measurement

The experimental setup for the ablation efficiency measurement is shown in Fig. 1. The ablation efficiency is the mass ablated per pulse per unit-of-laser-energy delivered. The ablated mass was determined by directly weighing the samples before and after ablation. Primary experimental results showed that a similar amount of clot could be removed using a 300-μm fiber either at 20 mJ during contact ablation or at 60 mJ during noncontact ablation. Consequently the noncontact experiments used three times the pulse energy that the contact experiments used. The pulse number varied from 180 to 395 depending on the removed mass that could be easily measured. The catheter was advanced manually during the procedure and five samples were ablated for each measurement. Nonlaser controls were exposed to flowing water or saline for about 2 min without irradiating, so that the mass lost due to the flowing fluid and the mass loss caused by mechanical manipulation could be assessed.

D. Flash Photography

Vapor bubble formation was visualized using flash photography (Fig. 2). Time zero corresponded to the rising edge of the signal from a photodiode attached to the laser delivery fiber. A digital delay generator (DG535, Stanford Research) was used to turn on a 5-μs strobe (MVS-2601, EG&G) at times ranging from 5 to 20 000 μs after the laser pulse. A triggerable CCD camera (CV-251, Protec) only recorded events illuminated by the strobe. The CCD image was captured with a video frame grabber (DT2255, Data Translation). Each picture recorded a single event and was repeated three times for each experiment. Single pulses of 10–25-mJ laser energy were delivered through a flushing catheter with a 300-μm diameter fiber for contact ablation. Noncontact ablation used 30–75-mJ laser pulses and the same fiber size.

E. Pressure Measurements

The pressure transients were measured with a piezoelectric polyvinlyidenefluoride (PVDF) transducer (KP 117, Ktech). The active square area of the transducer was 1 mm^2. The sensitivity was ~32 mV/bar and the rise time was ~400 ns. The transducer was factory calibrated in air to give absolute pressure amplitudes. However, the absolute pressures may be underestimated because the transducer was calibrated in air, but used in an aqueous environment. The acoustic signals were recorded on a digital storage oscilloscope (DSA 602A, Tektronix). The transducer was placed at a distance of ~16 mm from the target site under distilled water. The 1-mm flushing catheter with a 300-μm fiber was placed in a container filled with distilled water. The flow rate was 4 mL/min. Single pulses of 10–25 mJ were delivered onto the gelatin via a flushing catheter with a 300-μm fiber for contact ablation, and 30–75-mJ laser pulses were used for noncontact ablation.

F. Drug Delivery

Drug delivery using contact and noncontact methods was evaluated using 100-cm^{-1} gelatin targets. The gelatin samples were placed under distilled water at room temperature. A flushing catheter with a 300-μm fiber was used to deliver about 90 pulses with laser energies of 20 mJ (contact) and 50 mJ (noncontact) at 3 Hz perpendicularly onto gelatins. The catheter was advanced by hand as a channel was ablated through the gelatin. A 7.5×10^7 spheres/mL solution of 1-μm fluorescence spheres (Molecular Probes, Inc.) was infused at 4 mL/min during the ablation. The control samples were first ablated while water alone was infused at 4 mL/min. After a channel was created, the control samples were infused with the sphere solution for about 30 s. The number of laser pulses delivered were 95 ± 3 for contact and 93 ± 4 for noncontact.

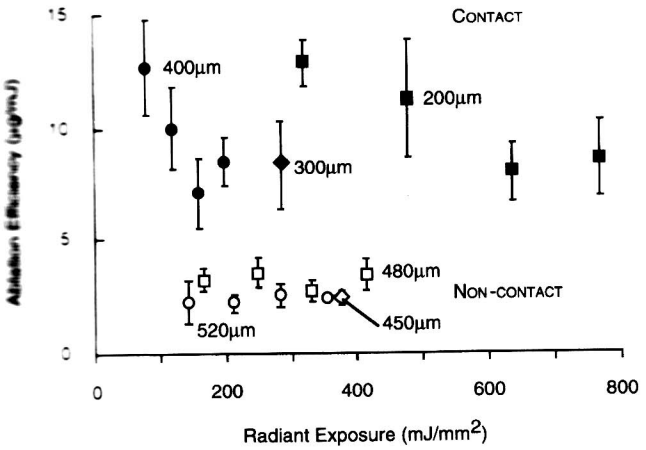

Fig. 3. Ablation efficiency of 1-μs laser pulses on clots from Pig B in Table II. The clot used was from a single pig. The filled markers are for contact ablation; noncontact ablation are presented with open markers. The laser spot sizes are labeled. All data are mean ± standard deviation of five samples.

All samples were carefully washed with clear water before being frozen and sectioned. Each frozen sample was cut into four or five sections with a thickness less than 100 μm. Frozen sections were examined under light and fluorescence microscopy. The penetration of the spheres in the gelatins was measured.

G. Statistical Analysis

All data is reported as mean ± standard deviation. The statistical significance of differences was determined using a two-tailed Student's t-test. An unpaired t-test was used to analyze the data as each parameter was varied. A value of $p < 0.05$ was considered to be significant.

III. Results

A. Ablation Efficiency of Porcine Clot

During ablation of the clot, a popping sound accompanied each laser pulse, and a stream of red liquid erupted along with some small particulates. The particulate size was correlated with white fibrin found in the clot. Smaller particulates were associated with more fibrin pieces. The number of fibrin chunks and the mechanical strength of the clots varied from pig to pig. Less mass was removed from the most durable clots. The rate of thrombus removal slowed as the clot became less red (presumably due to hemolysis and loss of hemoglobin). Smoke could be smelled at the highest laser energies (≥60 mJ) during noncontact delivery. The ablation efficiency (mass removed per unit energy) of contact ablation was at least three times greater than that of noncontact ablation (Fig. 3). There were no significant differences in the ablation efficiency at different spot sizes for either contact ablation or for noncontact ablation. Intra-animal variation significantly affected the ablation efficiency (Table II). No significant difference in the ablation efficiency of porcine clot under distilled water or normal saline was observed despite the fact that water can cause hemolysis.

TABLE II
VARIABILITY IN PORCINE CLOT ABLATION EFFICIENCIES. THE AVERAGE OF 180–350 20 mJ LASER PULSES DELIVERED THROUGH A 300-μm FIBER FOR CONTACT ABLATION AND 60 mJ LASER PULSES WERE USED FOR NON-CONTACT ABLATION. ALL DATA ARE MEAN ± STANDARD DEVIATION OF FIVE SAMPLES

PIG	ABLATION EFFICIENCY	
	Contact (μg/mJ)	Non-contact (μg/mJ)
A	14±2	4.7±1
B	8±2	2.4±0.3
C	7±1	—

B. Bubbles Evolution

Time-resolved flash photographs revealed that a laser pulse generated a cavitation bubble either at the fiber end or on the gelatin surface depending on where the laser energy was absorbed. Each picture was a single event and was repeated three times for each parameter set. The bubble size was reproducible to 5% before the bubble collapse. The appearance of cavitation bubbles varied widely after the bubble collapse.

Fig. 4 shows a compilation of the bubble expansion and collapse sequence in water for contact ablation. The maximum width of the bubble was ~2.8 mm and was reached at 75 μs. The bubble completely collapsed 250 μs after the laser pulse. Significant mass removal was observed at 275 μs and at 700 μs, respectively. Fig. 5 shows the bubble evolution in water for noncontact ablation. The maximum width of the bubble measured 3.6 mm at 95 μs. The bubble completely collapsed about 300 μs after the laser pulse. Material removal lasted from 300–900 μs. Fig. 6 shows the bubble width measured from Figs. 4 and 5.

C. Bubble Pressure

A representative pressure trace for a laser pulse of 30 mJ delivered onto gelatin under water in noncontact ablation is shown in Fig. 7. The initial pressure peak was due to a thermoelastic expansion wave. The second peak at 300 μs was generated by the collapse of the cavitation bubble. The times were corrected to account for the time delay associated with the time it takes the acoustic signal to propagate from the ablation site to the transducer. We assume pressure signals travelled at 1500 m/s. The results of the acoustic transient measurements are summarized in Fig. 8. The pressure amplitudes of the bubble expansion and collapse were nearly equal for any particular experiment. Pressure was generated during the contact delivery at a rate of about 12 kPa/mJ and during noncontact delivery at 4 kPa/mJ.

D. Drug Delivery

The greatest penetration of fluorescence spheres in the gelatins was 247 ± 57 μm for contact delivery and 250 ± 63 μm for noncontact delivery. The number of the spheres in the gelatins was similar for both contact delivery and noncontact delivery under fluorescence microscopy.

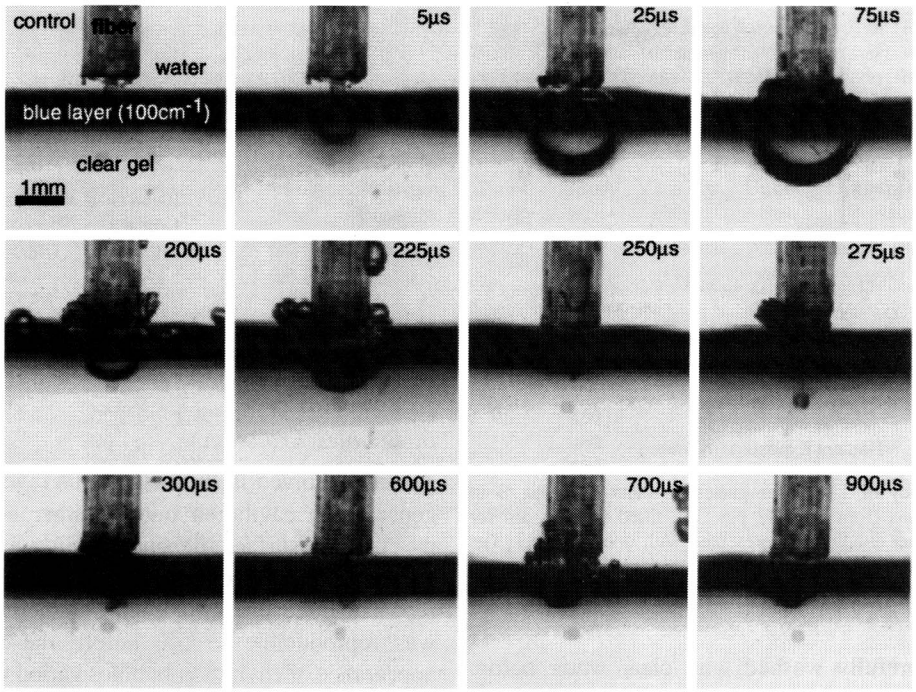

Fig. 4. Bubble formation on gelatin when the optical fiber is in contact with the gelatin surface. The optical fiber is centered in a 1-cm cuvette. A single pulse of 20 mJ laser energy was delivered through a flushing catheter with a 300-μm diameter fiber. The colored layer was 300 μm thick, but appears thicker due to a slight curvature of the surface.

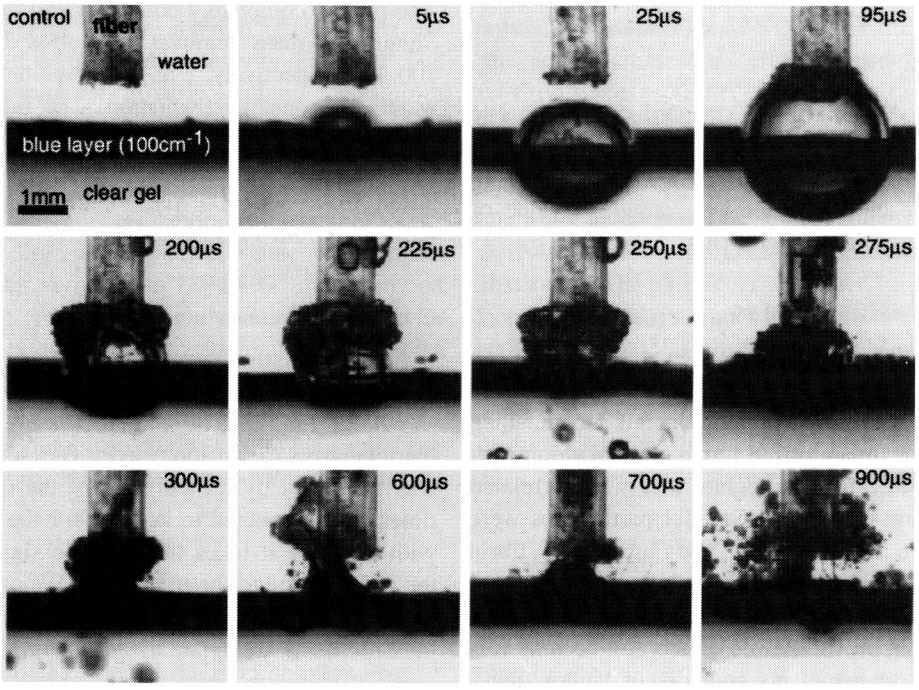

Fig. 5. Bubble formation on gelatin when the optical fiber is 2 mm above the gelatin surface. The optical fiber is centered in a 1-cm cuvette. A single 60-mJ laser pulse was delivered through a flushing catheter with a 300-μm diameter fiber. The colored layer was 300-μm thick.

IV. Discussion

Contact and noncontact ablation are remarkably similar when visualized using high speed photography (Figs. 4 and 5). A well-defined cavitation bubble is formed whether or not the fiber contacts the surface. The cavitation bubble grows and collapses; no secondary bubble is observed. Material removal follows the collapse of the bubble. When roughly equal size bubbles are formed, then the bubble lifetimes are also simila for contact and noncontact ablation.

Contact and noncontact ablation differs in a few ways Noncontact ablation forms a cavitation bubble that is hal inside the gelatin and half in the ambient liquid; the contac bubble creates a bubble that is nearly entirely containe within the gelatin. The shape of the noncontact bubble

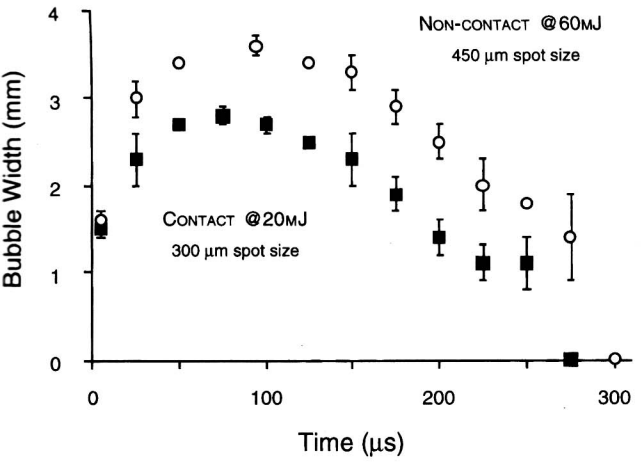

g. 6. Bubble width as a function of time after the laser pulse for the ontact and noncontact ablation, shown in Figs. 4 and 5. Error bars represent e standard deviation of three measurements.

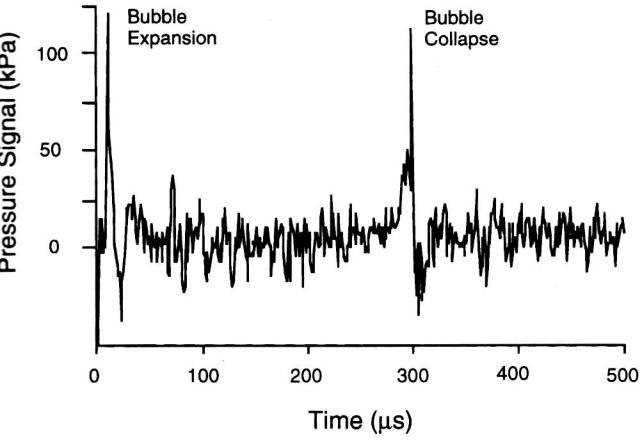

g. 7. The pressures induced by the cavitation bubble following laser adiation. The times have been corrected for the propagation delay of the essure signals from the ablation site to the pressure transducer.

t maximum size) is more spherical than contact ablation ubbles. Finally, there is some visual evidence that the contact blation removes material at two discrete times after the llapse of the cavitation bubble.

Quantitative measurements of the material removed during blation indicate that the ablation efficiency is profoundly ffected by whether or not the optical fiber tip directly contacts e thrombus. Noncontact ablation needed roughly three times much laser energy to remove the same amount of clot contact ablation needed (Table I). Similarly, the bubble xpansion pressures were nearly equal when the noncontact ser energy was three times the contact laser energy. A similar bservation was not observed for the maximum bubble size. oncontact ablation bubbles (at three times the energy) were rger than the contact bubbles.

The mass removed per unit energy (the ablation efficiency) as relatively constant for either contact or for noncontact ab- tion (Fig. 3). However, the ablation efficiency varied signif- antly when clots from different animals were ablated (Table). Furthermore, even the least efficient ablation (2.4 μg/mJ) as significantly greater than that would be expected from

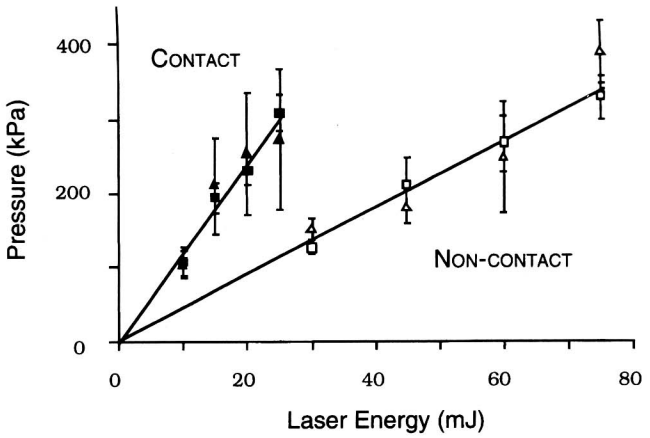

Fig. 8. Amplitude of the expansion and collapse pressures at a distance of 16 mm from the ablation site. The laser pulses were delivered onto the gelatin via a flushing catheter with a 300 μm fiber. The filled square and triangle are the pressures for contact ablation due to the bubble expansion and collapse respectively. The corresponding noncontact data is represented using the open markers. Error bars represent the standard deviation of six measurements.

a simple vaporization argument. The heat of vaporization of water is about 2.5 kJ/gm and so ablation that is solely due to vaporization would remove clot at a rate of 0.4 μg/mJ of laser energy. Consequently, the ablation process must be accompanied by mechanical disruption of the clot [16]. This was confirmed by flash photography.

Somewhat surprisingly, the mass removed per pulse did not depend on the spot size for either contact or noncontact ablation. The spot size plays an important role in ablation at pulse energies near the threshold for ablation [19]. In our experiments the ablation threshold was about 15 mJ/mm^2. Since the lowest radiant exposure was about 80 mJ/mm^2 or more than five times the ablation threshold, we must conclude that spot size plays only a secondary role at pulse energies significantly above threshold. In other words, it is not where the energy is deposited, but rather how much energy is deposited that affects the mass removal process.

Typically, a channel could be easily created through clot during either contact or noncontact laser ablation. The residual clot on the walls of the vessel (mural thrombin) was not so easily removed and white fibrin chunks always remained. This mural fibrin residue could be a potent stimulus for rethrombosis *in vivo*. Consequently, we measured the ability of the 50-mJ noncontact ablation and 20-mJ contact ablation to drive microspheres (to simulate a thrombolytic drug) into clot. The microspheres penetrated the mural clot the same distance for both ablation methods and suggests that either method might be used for localized drug delivery to enhance the thrombolysis process.

The expansion pressures generated by contact delivery (on gelatin) were similar to those during noncontact delivery at three times the pulse energy (Fig. 8). Moreover, for a given expansion pressure the contact bubbles were slightly smaller than the noncontact bubbles (Table I). This is evidently a consequence of noncontact bubbles being able to grow more easily in the less viscous fluid over the gelatin. Contact ablation achieved higher bubble expansion pressures for a given pulse energy due to the presence of the boundary of the fiber tip

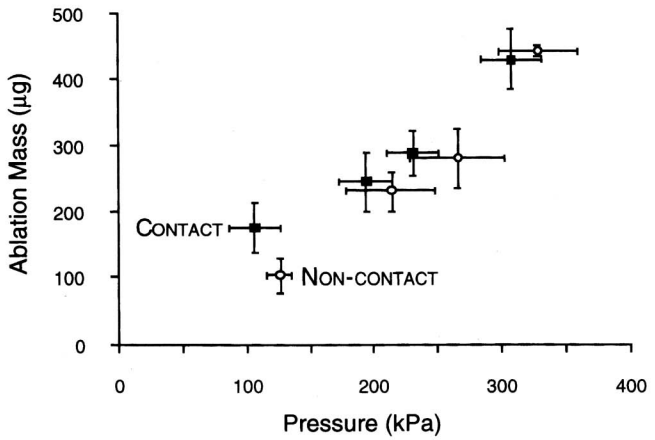

Fig. 9. Ablation mass of clot as a function of bubble expansion pressure on gelatin. The pressures were measured from gelatin samples with an absorption coefficient of 100 cm^{-1}. Single pulses of 10–25 mJ were delivered onto the gelatin samples via a 300-μm fiber for contact ablation, while noncontact ablation used energies three times those used for contact ablation. The ablation mass of clot from Pig A in Table II was measured using the same laser and fiber parameters used for the gelatin experiments.

[20]. The fiber tip constrains the direction that the initial cavitation bubble can travel—it must initially grow away from the fiber tip. This is sometimes called constrained vaporization or tamping and has been used extensively exploited for the ablation of kidney stones [21].

To summarize, material removal increased with increasing bubble size, increasing energy, and increasing pressures. Material removal did not change with spot size. When mass removal is plotted as a function of bubble size and pulse energy, two distinct groups of data result: one for contact and one for noncontact. However, when the mass ablated (for clot) is plotted as a function of the bubble expansion pressure (for gelatin) the data for both contact and noncontact ablation is grouped together much more closely (Fig. 9). Consequently, we are led to the conclusion that the most important parameter in microsecond ablation of soft materials in an aqueous environment is the expansion bubble pressures. A similar observation was made by Tomaru *et al.* who showed a weak correlation between shockwaves and mass removal during contact pulsed-dye laser ablation of aortic tissue [22].

This study demonstrated that the contact ablation efficiency of porcine clot was at least three times greater than the noncontact ablation efficiency. Furthermore, the mass removed per unit laser energy was relatively constant for both laser energy and fiber size. The mass ablated was correlated with the expansion pressure of the cavitation bubble. This result provides an important piece of information for designing clinical clot ablation systems: pressure is the most important factor in establishing the ablation efficiency of a 1-ms laser pulse. For example, since the mass removed per pulse is (roughly) linearly related to the bubble expansion pressure, ten small laser pulses will remove the same amount as one large pulse with ten times the energy. This is important because previous studies have demonstrated that cavitation bubbles can structurally deform vessel walls and possibly lead to damage of the vessel walls [23], [24]. Since larger bubbles generate greater pressures, a greater number of smaller bubbles may allow safer, more controlled, laser ablation of clot in arteries.

ACKNOWLEDGMENT

The authors thank Dr. K. W. Gregory and A. Shearin for their generous support and advice during this project.

REFERENCES

[1] K. Gregory, "Laser thrombolysis," in *Interventional Cardiology*, vol. 2, E. J. Topol, Ed. Philadelphia, PA: Saunders, 1994, ch. 5, pp. 892–902.
[2] M. R. Prince, T. F. Deutsch, A. F. Shapiro, R. J. Margolis, A. R. Oseroff, J. T. Fallon, J. A. Parrish, and R. R. Anderson, "Selective ablation of atheromas using a flashlamp-excited dye laser at 465 nm," *Proc. Nat. Acad. Sci. USA*, vol. 83, pp. 7064–7068, 1986.
[3] M. R. Prince, T. F. Deutsch, M. M. Mathews-Roth, R. Margolis, J. A. Parrish, and A. R. Oseroff, "Preferential light absorption in atheromas *in vitro*," *J. Clin. Invest.*, vol. 78, pp. 295–302, 1986.
[4] G. M. LaMuraglia, R. R. Anderson, J. A. Parrish, D. Zhang, and M. R. Prince, "Selective laser ablation of venous thrombus: Implications for a new approach in the treatment of pulmonary embolus," *Laser Surg. Med.*, vol. 8, pp. 486–493, 1988.
[5] F. Litvack, "Excimer laser coronary angioplasty," in *Interventional Cardiology*, vol. 2, E. J. Topol, Ed. Philadelphia, PA: Saunders, 1994, ch. 5, pp. 841–866.
[6] O. Topaz, "Holmium: YAG coronary angioplasty: The multicenter registry," in *Interventional Cardiology*, vol. 2, E. J. Topol, Ed. Philadelphia, PA: Saunders, 1994, ch. 5, pp. 867–891.
[7] K. W. Gregory and R. R. Anderson, "Liquid core light guide for laser angioplasty," *IEEE J. Quantum Electron.*, vol. 26, pp. 2289–2296, 1990.
[8] R. Srinivasan, K. G. Casey, and J. D. Haller, "Subnanosecond probing of the ablation of soft plaque from arterial wall by 308-nm laser pulses delivered through a fiber," *IEEE J. Quantum Electron.*, vol. 26, pp. 2279–2283, 1990.
[9] G. H. M. Gijsbers, R. L. H. Sprangers, M. Keijzer, J. M. T. De Bakker, T. G. van Leeuwen, R. M. Verdaasdonk, C. Borst, and M. J. C. van Gemert, "Some laser-tissue interactions in 308 nm excimer laser coronary angioplasty," *J. Interven. Cardiol.*, vol. 3, pp. 231–241, 1990.
[10] T. Tomaru, H. J. Geschwind, G. Boussignac, F. Lange, and S. J. Tahk, "Comparison of ablation efficiency of excimer, pulsed dye, and holmium-YAG lasers relevant to shock waves," *Amer. Heart J.*, vol. 123, pp. 886–895, 1992.
[11] M. Buchelt, T. Papaioannou, M. Fishbein, W. Peters, C. Beeder, and W. S. Grundfest, "Excimer laser ablation of fibrocartilage: An *in vitro* and *in vivo* study," *Laser Surg. Med.*, vol. 11, pp. 271–279, 1991.
[12] G. H. M. Gijsbers, D. G. van den Brocke, R. L. H. Sprangers, and M. J. C. van Gemert, "Effect of force ablation depth for a XeCl excimer laser beam delivered by an optical fiber in contact with arterial tissue in saline," *Laser Surg. Med.*, vol. 12, pp. 576–584, 1992.
[13] W. S. Grundfest, F. Litvack, J. S. Forrester, H. J. C. Swan, T. Goldenberg, L. Morgenstern, M. Fishbein, I. S. McDermid, D. M. Rider, T. J. Pacala, and J. B. Laudenslager, "Laser ablation of human atherosclerotic plaque without adjacent tissue injury," *J. Amer. Coll. Cardiol.*, vol. 5, pp. 929–933, 1985.
[14] F. Litvack, W. S. Grundfest, T. Goldenberg, J. Laudenslager, T. Pacala, J. Segalowitz, and J. Forrester, "Pulsed laser angioplasty: Wavelength power and energy dependencies relevant to clinical application," *Laser Surg. Med.*, vol. 8, pp. 60–65, 1988.
[15] R. S. Taylor, L. A. J. Higginson, and K. E. Leopold, "Dependence of the XeCl laser cut rate of plaque on the degree of calcification, laser fluence, and optical pulse duration," *Laser Surg. Med.*, vol. 10, pp. 414–419, 1990.
[16] J. T. Walsh, Jr. and T. F. Deutsch, "Pulsed CO_2 laser ablation of tissue: Effect of mechanical properties," *IEEE Trans. Biomed. Eng.*, vol. 36, pp. 1195–1201, 1989.
[17] E. H. Schallen, C. C. Awh, and E. de Juan, Jr., "Rate-dependent nonlinear photoablation of ocular tissue at 308 nm," *Laser Surg. Med.*, vol. 15, pp. 99–106, 1994.
[18] Y. C. Fung, *Biomechanics-Mechanical Properties of Living Tissues*, 2nd ed. Berlin: Springer, 1993.
[19] U. S. Sathyam, A. Shearin, E. A. Chasteney, and S. A. Prahl, "Threshold and ablation efficiency studies of microsecond ablation of gelatin under water," *Laser Surg. Med.*, vol. 19, pp. 397–406, 1996.

0] R. S. Dingus, "Laser-induced contained-vaporization in tissue," in *Proc. SPIE Laser-Tissue Interaction III*, S. L. Jacques, Ed., vol. 1646, pp. 266–274, 1992.
1] K. Rink, G. Delacrétaz, and R. P. Salathé, "Fragmentation process of current laser lithotriptors," *Laser Surg. Med.*, vol. 16, pp. 134–146, 1995.
2] T. Tomaru, H. J. Geschwind, G. Boussignac, F. Lange, and S. J. Tahk, "Characteristics of shock waves induced by pulsed lasers and their effects on arterial tissue: Comparison of excimer, pulse dye, and holmium YAG lasers," *Amer. Heart J.*, vol. 123, pp. 896–904, 1992.
3] T. G. van Leeuwen, J. H. Meertens, E. Velema, M. J. Post, and C. Brost, "Intraluminal vapor bubble induced by excimer laser pulse causes microsecond arterial dilation and invagination leading to extensive wall damage in the rabbit," *Circulation*, vol. 87, pp. 1258–1263, 1993.
4] A. Vogel, S. Busch, K. Jungnickel, and R. Birngruber, "Mechanisms of intraocular photodisruption with picosecond and nanosecond laser pulses," *Laser Surg. Med.*, vol. 15, pp. 32–43, 1994.

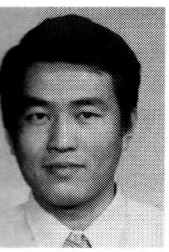

HanQun Shangguan received the B.Eng. degree in optical instrumentation from WuHan Institute of Surveying and Mapping, China, in 1982, and the M.S. and Ph.D. degrees in electrical engineering from Portland State University, Portland, OR, in 1993 and 1996, respectively.

From 1982 to 1990, he was an Engineer in China Nuclear Instruments and Equipment Co., China. He has been with Oregon Medical Laser Center since 1991. His current research interests are in light delivery systems for photodynamic therapy d tissue weld, fluorescence spectroscopy, laser-induced cavitation bubble namics, and drug delivery with microsecond laser pulses. He has over 20 earch publications.

Dr. Shangguan is a member of Eta Kappa Nu, SPIE, and the Optical ciety of America.

Lee W. Casperson (M'79–SM'83–F'94) received the B.S. degree in physics from the Massachusetts Institute of Technology, Cambridge, in 1966, and the M.S. and Ph.D. degrees in electrical engineering and physics from the California Institute of Technology, Pasadena, in 1967 and 1971, respectively.

From 1971 to 1983, he was a Faculty Member in the Department of Electrical Engineering at the University of California, Los Angeles, and since 1983, he has been with the Department of Electrical Engineering at Portland State University, Portland, OR. His current research interests are in lasers and optical systems. He has over 200 research publications.

Dr. Casperson was awarded the IEEE Centennial Medal and is a Fellow of the Optical Society of America.

Scott A. Prahl received the B.S. degree in physics from the California Institute of Technology, Pasadena, in 1982, and the Ph.D. degree in biomedical engineering from the University of Texas, Austin, in 1988.

From 1990 to 1991, he was an Instructor in Wellman Laboratories at Massachusetts General Hospital, Boston. Since 1992, he has been with the Oregon Medical Laser Center, the Department of Electrical Engineering, Oregon Graduate Institute, Portland, OR, and the Department of Dermatology, Oregon Health Sciences University, Portland, OR. His current research interests are in noninvasive measurement of subsurface temperature, visible and infrared spectroscopy of tissues, and tissue optics. He is the author of over 100 research publications.

Dr. Prahl was the recipient of the Dermatology Foundation Research Award. He is a Fellow of the American Society for Laser Medicine and Surgery.